ELSEVIER

Materials Science and Engineering B69–70 (2000) 361–366

MATERIALS SCIENCE & ENGINEERING B

www.elsevier.com/locate/mseb

# Computer-aided analysis of TEM images of CdSe/ZnSe quantum dots

H. Kirmse [a,*], W. Neumann [a], T. Wiebach [a], R. Köhler [a], K. Scheerschmidt [b], D. Conrad [b]

[a] *Humboldt University of Berlin, Department of Physics, Invalidenstrasse 110, D-10115 Berlin, Germany*
[b] *Max Planck Institute of Microstructure Physics, Weinberg 2, D-06120 Halle, Germany*

**Abstract**

Self-organized CdSe/ZnSe quantum dots (QDs) were investigated by means of transmission electron microscopy (TEM). Plan-view diffraction contrast images each obtained under individual diffraction conditions showed different contrast behaviour. Bright-field imaging of single dots revealed circle-like contrast features. In the $0\bar{4}0$ dark-field image a 2-fold symmetry and in the $\bar{2}20$ dark-field image a nearly 4-fold symmetry of the contrast features were observed. Supplementary strain-field calculations using a finite-element method were compared with the experimental contrast features. The distributions of the several strain components chosen according to the certain diffraction conditions show the same symmetry and orientation as the experimental features.


*Keywords:* Transmission electron microscopy; CdSe/ZnSe quantum dots; Self organization; Finite-element method; Lattice mismatch; Strain

## 1. Introduction

Quantum structures like quantum wells, quantum wires, and quantum dots are of great fundamental and technological interest because of their physical properties, especially as to their optoelectronical behaviour. Quantum dots (QDs) are structures limited in the three spatial directions to only some nanometers where quantum-size effects become important. Besides the III–V materials like (In,Ga)As/GaAs or (In,Ga)P/InP yielding infrared and red light emission II–VI materials like CdSe/ZnSe were found to form QD structures of emission in the blue–green range.

The formation of QDs on non-structured surfaces is a self-organization process due to the lattice mismatch being about 7% for CdSe/ZnSe. In general, there are three possible modes of the growth of mismatched structures. Pseudomorphic layer growth is described by the model of Frank and van der Merwe [1], where the relaxation of strain is realized by strained unit cells and after exceeding a critical thickness by the generation of misfit dislocations or surface modulation. The generation of islands on a wetting layer having the critical thickness for strain relaxation was predicted by Stranski and Krastanow [2]. Hereby, the strain is predominantly relaxed in the upper regions of the islands. Volmer and Weber [3] described the immediate growth of isolated islands on the substrate without the presence of a wetting layer.

The self-organization process of the CdSe/ZnSe is similar to the Stranski–Krastanow growth mode established for the III–Vs. But, in contrast to that an additional activation energy is mandatory for the reorganization of the top atomic layer to 3-dimensional islands. This was shown by Rabe et al. [4] for growing CdSe in a layer by layer mode on (001) ZnSe. The CdSe/ZnSe QDs were formed during an intermediate annealing step adapted to the molecular beam epitaxy (MBE) growth process. A two monolayers (MLs) thick remnant layer was verified by X-ray diffraction experiments [5].

Transmission electron microscopy (TEM) investigations were applied in order to study the structural and chemical properties of the QDs. Plan-view diffraction contrast imaging reveal contrast features having 4-fold symmetry hinting to entities having a 4-fold symmetry, too [6]. A size distribution of 5–50 nm and an average area density of 100 $\mu m^{-2}$ were found. Respective cross-

* Corresponding author. Tel.: +49-30-2093-7641; fax: +49-30-2093-7760.
*E-mail address:* holm.kirmse@physik.hu-berlin.de (H. Kirmse)

0921-5107/00/$ - see front matter 
PII: S0921-5107(99)00294-9

sectional examinations were carried out by diffraction contrast as well as high-resolution TEM (HRTEM) imaging. The HRTEM inspections and subsequent image analysis yielded a height of about 3 nm and a projected width of about 15 nm. Information about the chemical composition was obtained by energy dispersive X-ray spectroscopy (EDXS) [7], which revealed a clearly wider Cd distribution in the QD region of about 5.5 nm compared to the adjacent CdSe wetting layer where 2.5 nm were found. The larger values in comparison to the HRTEM results were attributed to beam broadening and secondary fluorescence.

Computer-aided image-contrast simulations necessary for a reliable interpretation of the diffraction contrast images are in good agreement with the experiments for a truncated pyramid having {101} facets and with the edges of its basal plane orientated parallel to the ⟨100⟩ directions [7,8]. An ⟨110⟩ orientation and {111} or {113} facets yielded contrast features rotated by 45° in comparison to the experimental one. Furthermore, finite-element method (FEM) calculations utilizing the linear elasticity theory were applied to describe the strain field surrounding the CdSe/ZnSe QDs. The maximum of the atomic displacement found at the edges of the basal plane explained the bright-field contrast features visible in the experiment exhibiting maximum dark contrast along these edges [8].

## 2. Experimental

The quantum structures were grown by MBE on (001) GaAs. Details of the growth procedure are given in [4]. The large thermal misfit between ZnSe and GaAs causes misfit dislocations. In order to supply a structurally perfect surface a 1 μm thick ZnSe buffer layer was grown. The two-dimensional layer by layer growth of ZnSe at a temperature of 310°C was monitored by reflection high energy electron diffraction (RHEED). After lowering the substrate temperature to 230°C 3 MLs of CdSe were deposited again in a layer by layer mode making the CdSe thickness controllable by means of the RHEED intensity oscillations. Subsequent increasing the substrate temperature to 310°C and waiting for some seconds causes a significant change of the shape of the RHEED spots from initially streaky to spotty indicating the formation of 3-dimensional structures. Finally the CdSe was capped by an 85 nm thick ZnSe layer.

The preparation of TEM samples in plan view comprised a mechanical pre-thinning down to a thickness of about 100 μm, cutting discs out of the wafer, dimpling ending up with a thickness of about 30 μm and finally $Xe^+$ ion milling always from the back to preserve the quantum structure. The ion milling was carried out by applying a gradual reduction of the acceleration voltage from 5 to 0.7 kV in order to minimize preparation artifacts like micro-twins.

The TEM investigations were performed on an HITACHI H-8110 microscope (200 kV) equipped with the standard double-tilt holder.

For the FEM calculations of the strain field surrounding the QDs the software package MARC was used. The existence of defect-free islands confirmed by the cross section HRTEM investigations [6] allows to apply the linear elasticity theory. For the FEM calculations a sample setup has to be created and divided into small units having almost the same materials properties namely the same elastic constants. On a 5 nm thick and 15 × 15 nm wide ZnSe base an 1 nm thick ZnSe wetting layer was defined. Two assumptions were made for setting up a CdSe island. In the first model only a complete CdSe pyramid having {101} facets and with the edges of its basal plane orientated along ⟨100⟩ directions was placed on the ZnSe wetting layer. In the second model this pyramid was truncated at a height of 1.5 nm according to the findings of the diffraction contrast simulations and finally it was covered by a 5 nm thick ZnSe cap.

## 3. TEM diffraction contrast investigations

Fig. 1 shows the results of the plan-view TEM investigations. From Fig. 1a, where a representative bright-field image taken along the [001] zone axis is given, the size of the individual contrast features can be estimated to be about 20 nm or even smaller. Because the diffraction contrast of the QDs is mostly influenced by the strain field in their surrounding consequently the QD size is overestimated. The contrast feature near the center of the image (marked by an arrow) shows a continuous dark ring indicating the strain field. Here, contributions to the contrast are present from all the lattice planes taking part in the diffraction process, therefore, a circle-like contrast is imaginable. The corresponding $0\bar{4}0$ dark-field image of the same area is given in Fig. 1b. Under the imaging condition chosen all contrast features exhibit a 2-fold symmetry (see e.g. the marked ones) due to the strain induced distortion of the 040 lattice planes. The $\bar{2}\bar{2}0$ dark-field image of Fig. 1c partly reveals a substantial different contrast behaviour (cf. the marked feature). Two lines of no contrast orientated parallel to the ⟨100⟩ directions intersect in the central region of the contrast feature. Apparently the distortion of the 220 lattice planes in the QD region is of nearly four-fold symmetry. Fig. 1d shows the respective selected area diffraction pattern along the [001] zone axis with the positions of the aperture indicated used for the individual imaging condition. The findings of the TEM diffraction contrast investigations have to be verified by respective strain-field simulations

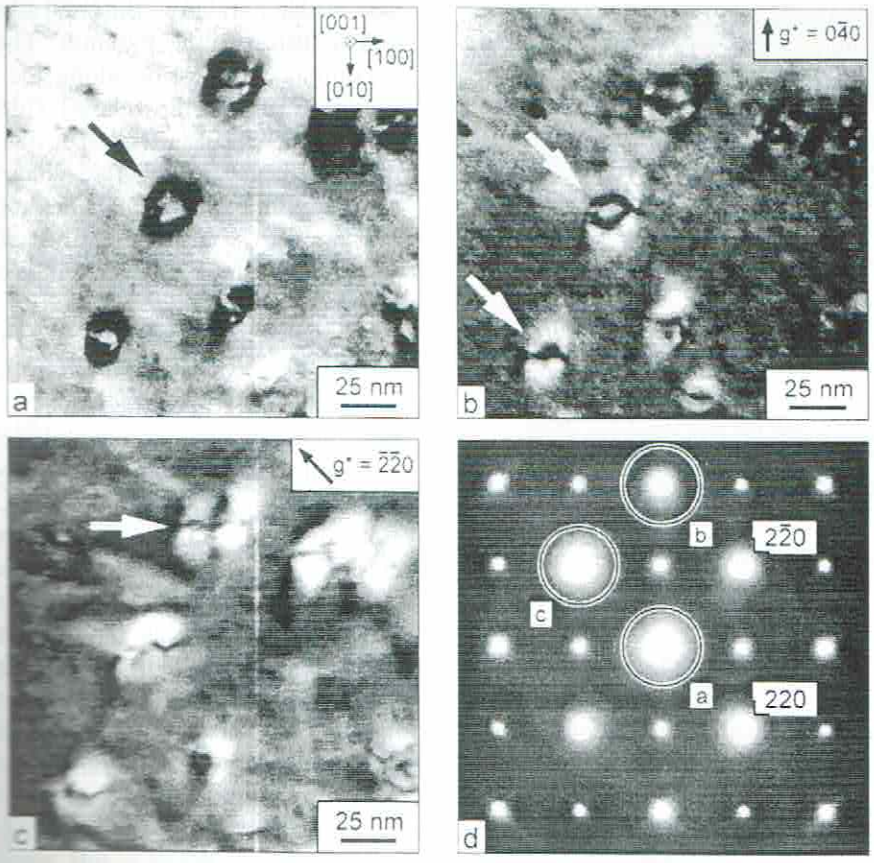


Fig. 1. Plan-view transmission electron microscopy (TEM) images of CdSe/ZnSe quantum dots (QDs): (a) diffraction-contrast bright-field images; (b) 040 dark-field image; (c) $\bar{2}20$ dark-field image; and (d) selected-area diffraction pattern with the reflections chosen for imaging marked by circles.

utilizing the FEM, the results of which are presented in the following.

## 4. FEM strain-field calculations

The evaluation of the strain field surrounding the CdSe/ZnSe QDs requires the application of FEM. Two basic structure models were created, the less complex one is schematically drawn in Fig. 2. The length of the [100] edges of the basal plane of the CdSe pyramid was defined to be 5 nm. This value corresponds to the smallest contrast features found, the strain distribution is the same as for larger pyramids. The plane used for the following representations of the strain field is marked by the bold lines. It cuts the initial model at the surface of the CdSe wetting layer and at the bottom of the pyramid where in cross-sectional strain-field calculations the maximum elastic strain energy was found [8]. Attributed to the strain the surface of the wetting layer is raised and consequently the cutting plane resides underneath the surface.

In Fig. 3 the elastic strain energy density is given, where high density is denoted by high brightness. The dark lines visible connect the nodes defined for the FEM procedure. The drawing represents almost all the strain affecting the bright-field diffraction contrast. The highest elastic strain energy density is found at the edges of the basal plane causing the contrast feature of Fig. 1a. The lowest density is determined at the central region of the basal plane indicating the high efficiency of the island formation for the relaxation of strain. The medium gray level outside the pyramid indicates the residual strain away from the islands.

In Fig. 4 the components of the elastic strain in several directions are presented and an interpretation of the results is given. Fig. 4a depicts the strain compo-

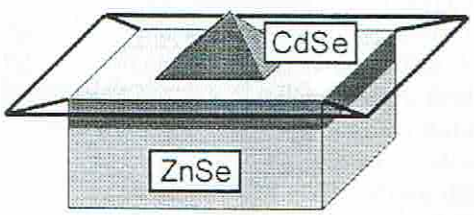


Fig. 2. Sample setup for the finite-element method (FEM) strain-field calculations for the complete uncovered pyramid. The cutting plane referred to in the following pictures is marked.

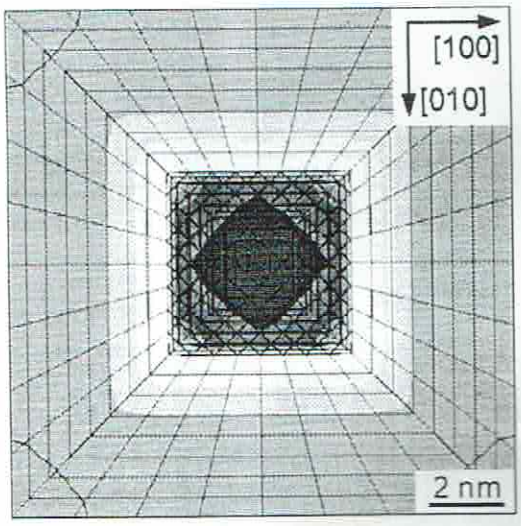


Fig. 3. Elastic strain-energy at the basal plane of the pyramid. High brightness indicates high strain-energy density.

nent parallel to the [010] direction. This strain directly affects the distortion of the 040 lattice planes which contribute to the image contrast of Fig. 1b. The maximum compressive strain is marked by minimum brightness visible parallel to the [100] edges of the basal plane and a little off the pyramid. The appearance of the maximum compression along the edges is due to the superposition of the relaxed CdSe pyramid and the pseudomorphically strained CdSe wetting layer. The material inside the pyramid tends to relax at the base edges too, but the wetting layer acts against causing the maximum of strain. In contrast to that the maximum elongation is found at the center of the pyramids base attributed to the relaxation.

The [010] strain component exhibits a two-fold symmetry which was also realized in Fig. 1b. The impact of this strain on an arbitrary defined square-like unit cell is sketched in Fig. 4b. The unit cells at the [100] edges are compressed parallel to [010] labeled by dark arrows. Unlike to that the unit cells at the [010] edges are elongated in [010] direction (cf. bright arrows). In conclusion, a 2-fold symmetry is obvious.

Fig. 4c represents the elastic strain parallel to the [110] direction causing the diffraction contrast of Fig. 1c. In the simulation the maximum and the minimum values are found at the corners of basal plane. The drawing of Fig. 4d helps to clarify the findings. The initially square-like unit cells are distorted to rhombi.

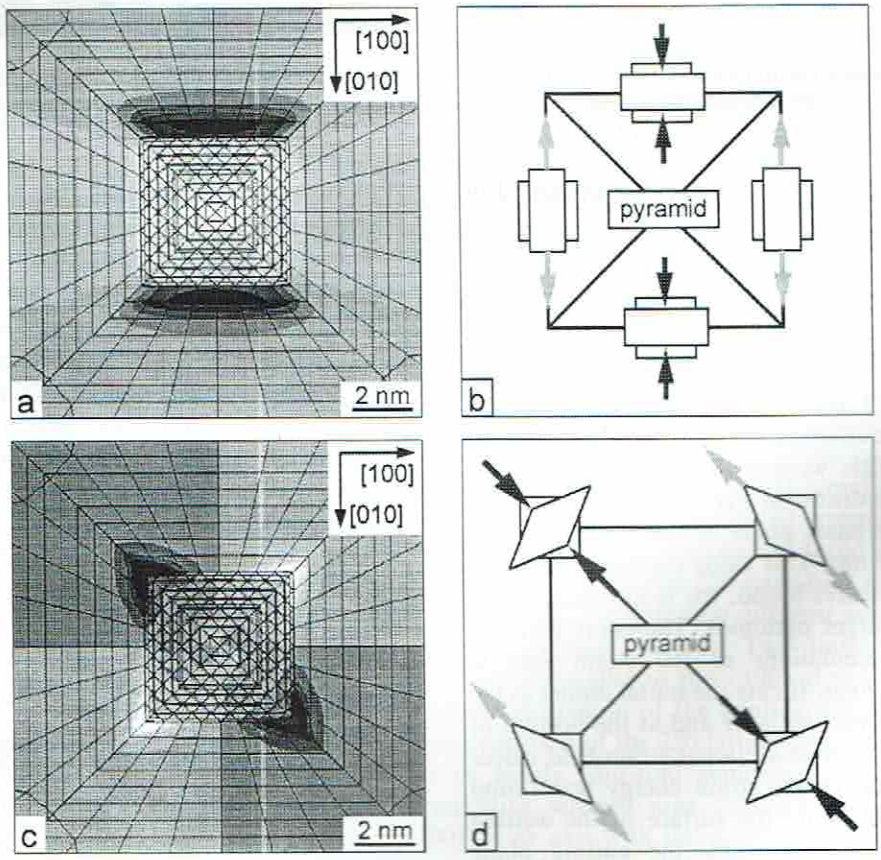


Fig. 4. Finite-element calculations of the strain field surrounding the quantum dots (QDs): (a) [010] component of the elastic strain; (b) visulaization of the deformation parallel to the [010] direction of initially square-like unit cells at the edges of the basal plane; (c) [110] component of the elastic strain; and (d) deformation along the [110] direction at the corners of the pyramids base.

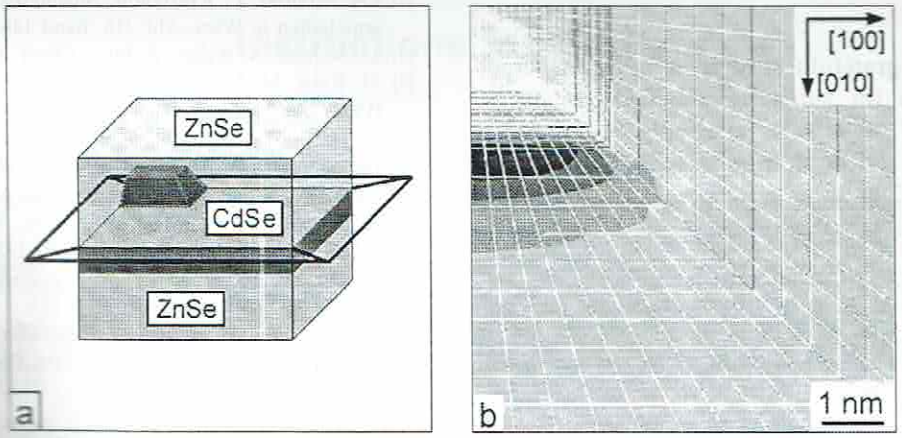


Fig. 5. Finite-element method (FEM) calculations for a truncated tetragonal CdSe pyramid capped with ZnSe: (a) sample setup with the cutting plane marked; (b) distribution of the [010] component of the elastic strain. Due to the 4-fold symmetry only a quarter of the pyramid is shown.

Concerning the strain along [110] a compression is found near the upper left and the lower right corner of the basal plane and an elongation is found near the upper right and the lower left corner.

The contrast behaviour in diffraction contrast images depends on the lattice planes involved in the diffraction process. No image contrast arises if lattice planes have homogeneous distances. But, a local deviation from the mean lattice constant, i.e. a slightly different fulfillment of the diffraction condition leads to a local change of the intensity, namely to the diffraction contrast observable.

In the experimental $\bar{2}20$ dark-field image of the CdSe QD given in Fig. 1c a higher brightness is visible at the corner regions of the basal plane. In the respective bright-field image with only the 000 and the $\bar{2}20$ reflections excited the contrast behaviour has to be inverted. Therefore, in the bright-field image the diffraction condition is less satisfied in the corner regions of the basal plane due to the distortion of the lattice planes. This results in a four-fold symmetry and provides an explanation for the findings of the TEM investigations by means of the FEM calculations.

In order to approximate the experimental situation as close as possible the setup for the FEM calculations was modified by introducing a truncation of the pyramid at a height of 1.5 nm and capping with 5 nm ZnSe. The improved sample setup is given in Fig. 5a. Because of its 4-fold symmetry the size of the model was reduced to 0.25. The cutting plane remains the same like in the uncapped case (see bold lines). In Fig. 5b the distribution of the [010] component of the elastic strain is shown. Comparing Fig. 5b and Fig. 4a both showing the same strain component one can see that there is no big difference of the strain distribution. In both viewgraphs the maximum of strain is determined at the edges of the basal plane. Unlike to that the maximum of compression is a little bit closer to the edge of the capped pyramid. Therefore the size of the capped pyramids can be estimated roughly as the same which is concluded from contrast feature.

## 5. Conclusions

TEM investigations of CdSe/ZnSe QDs grown by a modified MBE growth regime were performed by plan-view diffraction contrast under different imaging conditions. Viewing in bright-field along the [001] zone axis revealed a contrast feature behaving like a closed circle. Using the dark-field information of the $0\bar{4}0$ and the $\bar{2}20$ reflections a 2-fold and a 4-fold symmetry, respectively, were observable. The size of the QDs estimated from the individual contrast feature was found to be about 20 nm. The contrast behaviour could be explained by strain-field calculations utilizing FEM. These simulations are based on two structure models which differ in their complexity. One model consisted of an uncapped complete CdSe pyramid on a CdSe wetting layer placed on the ZnSe substrate and the other one of a truncated CdSe pyramid capped by ZnSe. The total strain-energy distribution is an appropriate measure of the strain influence on the bright-field image. Its maximum shows a closed ring behaving square-like symmetry similar to that found in the experimental image. The 2- and the 4-fold symmetry of the experimental dark-field contrast features closely correspond with the distribution of the [010] and the [110] strain components calculated by FEM. The comparison of the elastic strain distribution of the two different structure models revealed a strong similarity permitting the conclusion of a weak influence of the capping layer on the symmetry of the strain field in the surrounding of the QDs.

## Acknowledgements

The authors are grateful to Professor F. Henneberger and Dr M. Rabe for supplying the QD structures. H.K., W.N., T.W. and R.K. gratefully acknowledge financial support in the framework of the Sonderforschungsbereich 296.

## References

[1] F.C. Frank, J.H. van der Merwe, Proc. R. Soc. Lond. A 198 (1949) 205.
[2] I.N. Stranski, L. Krastanow, Sitzungsberichte d. Akad. d. Wissenschaften in Wien, Abt. IIb, Band 146 (1937) 797.
[3] M. Volmer, A. Weber, Z. Phys. Chem. 119 (1926) 277.
[4] M. Rabe, M. Lowisch, F. Henneberger, J. Cryst. Growth 185 (1998) 248.
[5] M. Rabe, M. Lowisch, F. Kreller, P. Schäfer, T. Flissikowski, F. Henneberger, in: D. Gershoni (Ed.), Proc. 24th ICPS Conf., Jerusalem, World Scientific, Singapore, 1998, CD-ROM.
[6] H. Kirmse, R. Schneider, M. Rabe, W. Neumann, F. Henneberger, Appl. Phys. Lett. 72 (1998) 1329.
[7] H. Kirmse, R. Schneider, K. Scheerschmidt, D. Conrad, W. Neumann, J. Microsc. 194 (1999) 183.
[8] W. Neumann, H. Kirmse, R. Schneider, K. Scheerschmidt, D. Conrad, T. Wiebach, R. Köhler, Inst. Phys. Conf. Ser. (1999), in print.